Catalytic Synthesis of Ti_2S Nanofibers

C. H. Liang,* G. W. Meng, G. Z. Wang, and L. D. Zhang

Department of Nanostructured Materials and Laboratory of Internal Friction and Defects in
Solids, Institute of Solid State Physics, Chinese Academy of Sciences,
Hefei 230031, P. R. China

S. Y. Zhang

Structure Research Laboratory, University of Science and Technology of China,
Hefei, 230026, P. R. China

Received December 29, 2000. Revised Manuscript Received February 24, 2001

Dititanium sulfide (Ti_2S) nanofibers were synthesized through chemical reactions from gaseous reagents of $TiCl_x$, H_2S, and S with the help of Ni catalysts at elevated temperature (950 °C). Highly dispersed Ni nanoparticles and H_2S (or S) gases were obtained by decomposing the preintroduced $NiSO_4$ nanoparticles confined in the pores of activated carbon in a reducing H_2 atmosphere. The active Ni catalyst provides an energetically favored site for the absorption of gaseous $TiCl_x$, H_2S, and S to form an ultrafine liquid alloy droplet containing Ti and S atoms. Then a vapor−liquid−solid growth was involved in the formation of Ti_2S nanofibers. SEM and TEM investigations show that the Ti_2S crystals grew in the form of nanofibers with diameters mainly around 20∼50 nm and lengths up to several tens of micrometers. Most Ti_2S nanofibers have smooth surface with a quadrilateral, triangular, or hexagonal cross section, while the others have a wavy appearance.

Introduction

Since the pioneering work by Iijima in making carbon nanotubes in 1991,[1] the fabrication or synthesis of one-dimensional (1D) nanostructures has drawn much attention due to their potential applications in mesoscopic research, nanostructured composite materials, and the development of nanodevices. Transition-metal chalogenides including sulfides, selenides, and tellurides are often found in minerals and have attracted considerable attention in recent decades due to their commercial applications in pigments, lubricants, fluorescence devices, and even superconductors.[2,3] Recently, fullerene-like nanoparticles or nanotubes of transition-metal sulfides, such as WS_2 and MoS_2, have been successfully synthesized by annealing oxidized transition-metal films in a stream of H_2S gas[4] or by chemical transport reactions.[5] However, aside from the above two compounds, little has been reported on the synthesis of other 1D nanostructures of transition-metal sulfides. Titanium sulfides are nonstoichiometric compounds that have commercial applications in dry lubrication, semiconductors, and energy batteries.[6] Because of the effect of the 3d electrons, titanium sulfides have many different phases compositions such as S-rich TiS_2, TiS_3, and Ti-rich Ti_2S.[7] Recently, Martin and co-workers have succeeded in fabricating TiS_2 microtubular battery electrodes by chemical vapor deposition using a template method.[8] As for sulfides in the Ti-rich side, one kind of titanium sulfide with the formula of Ti_2S was first found as an inclusion phase isolated from the Cr−Ni−Ti steel by electrolytic extraction in 1957.[9] Since then, Ti_2S crystals have also been synthesized by the reactions between TiS and Ti in a sealed tube heated at 1000 °C or Ti and S powders at 800∼1000 °C. However, only Ti_2S gray powders could be obtained.[10] From previous studies,[11,12] it could be seen that most nanostructures, such as nanowires or nanotubes, could be synthesized with the help of transition metals as

---

* To whom correspondence should be addressed. Fax: 0551-5591434. E-mail: chliang@mail.issp.ac.cn.

(1) Iijima, S. *Nature* **1991**, *354*, 56.

(2) Stuczynski, S. M.; Know, Y. U.; Steigerwald, M. L. *J. Organomet. Chem.* **1993**, *449*, 167.

(3) Nickless, G. *Inorganic Chemistry of Sulfur*; Elsevier: London, 1968, p 670. Greenwood, N. N.; Earnshaw, E. A. *Chemistry of the Elements*; Pergamon: Oxford, 1990; p 1403.

(4) Tenne, R.; Margulis, L.; Genut, M.; Hodes, G. *Nature* **1992**, *360*, 444. Feldman, Y.; Wasserman, E.; Srolovitz, D. J.; Tenne, R. *Science* **1995**, *267*, 111. Tenne, R. *Adv. Mater.* **1995**, *7*, 965. Zhu, Y. Q.; Hsu, W. K.; Grobert, N.; Chang, B. H.; Terrones, M.; Terrones, H.; Kroto, H. W.; Walton, R. M. *Chem. Mater.* **2000**, *12*, 1190.

(5) Remskar, M.; Skraba, Z.; Cléton, F.; Sanjinés, R.; Lévy, E. *Appl. Phys. Lett.* **1996**, *69*, 351. Remskar, M.; Skraba, Z.; Cléton, F.; Sanjinés, R.; Lévy, E. *Appl. Phys. Lett.* **1999**, *74*, 633. Remskar, M.; Skraba, Z.; Ballif, Z.; Sanjinés, R.; Lévy, E. *Surf. Sci.* **1999**, *435*, 637.

(6) Bonneau, P. R.; Jarris, R. R., Jr.; Kaner, P. B. *Nature* **1991**, *349*, 510. Finkman, E.; Fisher, B. *Solid State Commun.* **1984**, *51*, 25. Ferrer, I. J.; Caballero, F.; Delas, H. C.; Sarchez, C. *Solid. State. Commun.* **1994**, *89*, 349.

(7) Wittingham, M. S. *Science.* **1976**, *192*, 1126. Haraldsen, H.; Kjekshus, A.; Rost, E.; Steffensen, A. *Acta Chem. Scand.* **1963**, *17*, 1283. Owens, J. P.; Conard, B. R.; Franzen, H. F. *Acta Crystallogr.* **1967**, *23*, 77.

(8) Che, G.; Jirage, K. B.; Fisher, E. R.; Martin, C. R.; Yoneyama, H. *J. Electrochem. Soc.* **1997**, *144*(12), 4296.

(9) Brown, J. F.; Clark, W. D.; Parker, A. *Metallurgia* **1957**, *56*, 223.

(10) Whittingham, M. S.; Panella, J. A. *Mater. Res. Bull.* **1981**, *16*, 37. Thompson, A. H.; Gamble, F. R.; Symon, C. R. *Mater. Res. Bull.* **1975**, *10*, 915.

(11) Givargizov, E. I. *J. Vac. Sci. Technol., B* **1993**, *11*, 449; Duan, X. F.; Wang, J. F.; Lieber, C. M.; *Appl. Phys. Lett.* **2000**, *76*, 116. Yazawa, M.; Koguchi, M.; Muto, A.; Hiruma, K. *Adv. Mater.* **1993**, *5*, 577.

10.1021/cm001421i CCC: $20.00

catalysts. In this work, we present an experimental evidence for the formation of dititanium sulfide (Ti_2S) 1D nanostructures via a vapor–liquid–solid (VLS) growth catalyzed by Ni nanoparticles. The in situ generated Ni catalysts from the decomposition of $NiSO_4$ nanoparticles in a H_2 atmosphere provide active sites for the dissolution of Ti and S atoms from the gas reagents of $TiCl_x$, H_2S, and S. Then Ti_2S crystals precipitate from a supersaturated liquid alloy droplet with anisotropic growth.

Experimental Section

Materials. Activated carbon cylinders (commercial product) were immersed in a 0.25 M $NiSO_4$ solution (100 mL) for four weeks in a sealed glass vessel. The activated carbon would readily absorb the solution through capillary action, and then the $NiSO_4$ impregnated activated carbon cylinders were subjected to drying at 150 °C for 10 h to remove the residue solvents, leaving the $NiSO_4$ nanoparticles sequestered in the pores. Thus the highly dispersed $NiSO_4$ nanoparticles confined in the pores of activated carbon were obtained, which is analogous to the method used in the synthesis of SiC nanorods.[13]

Synthesis. The preparation of Ti_2S nanostructures was carried out in a horizontal furnace. A ceramic boat loaded with the obtained activated carbon containing $NiSO_4$ nanoparticles was placed into a quartz tube. The reaction chamber was evacuated by using a mechanical pump before flowing high-purity Ar gas (0.1MPa, 30sccm) was introduced, and then the chamber was heated. As soon as the temperature reached 950 °C (within 11 min), a gaseous mixture of $TiCl_4$ and dry H_2 (160 mL/min) was introduced; the chamber was maintained at this temperature for 1.5 h. After the run was over, the mixture reaction gases were switched off and high-purity Ar (1500 mL/min) was introduced into the chamber again until the chamber cooled to room temperature. A layer of light black, wool-like product was collected on the surface of the activated carbon cylinders for further analysis.

Characterization. The synthesized product was characterized using an X-ray diffraction spectrometer (XRD) (MAC SCIENCE MXP18AHF, Cu Kα radiation, $\lambda = 1.54056$ Å), a transmission electron microscope (TEM) (JEOL-2000 FX, 200 kV), a high-resolution transmission electron microscope (HRTEM) (JEOL-2010, 200 kV) attached to an energy-dispersive X-ray spectrometer (EDX) (OXFORD, Link ISIS), and a scanning electron microscope (SEM) (JEOL JSM-6300, 30 kV) attached to an EDX (Kevex, Sigama). For TEM observation, the specimen was prepared by enclosing a small piece of the product in a double copper grid without a support membrane. For HRTEM observation, the product was ground in a mortar and ultrasonically dispersed in ethanol; a drop was then dipped onto carbon-coated Cu microgrids. The SEM sample was presputtered with a layer of conducting Pt metal.

Results and Discussion

XRD. The as-prepared product was characterized by X-ray powder diffraction (Figure 1). It can be seen that all the peaks can be indexed to the hexagonal Ti_2S phase with lattice constants of $a = 3.206$ Å and $c = 11.19$ Å, which was in good agreement with reported values in the literature.[14] No other impurities were detected in the XRD pattern.

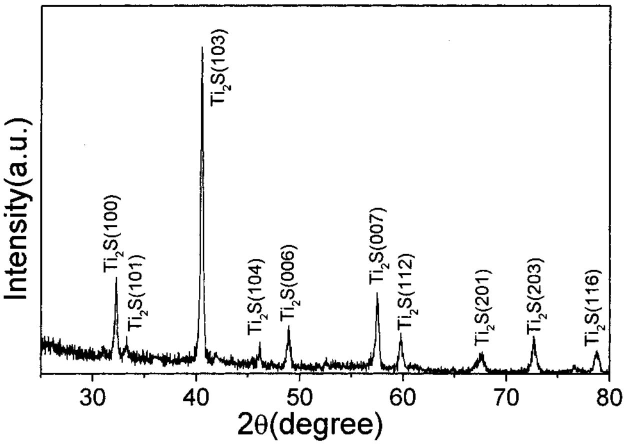

Figure 1. X-ray diffraction pattern of the synthesized Ti_2S nanofibers.

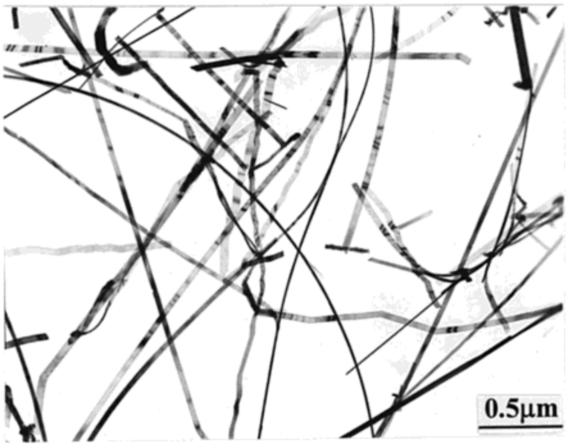

Figure 2. Low-magnified TEM image of the randomly displayed Ti_2S nanofibers.

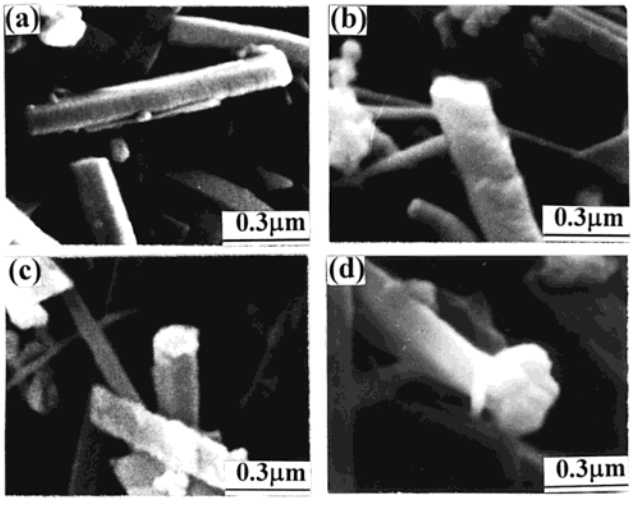

Figure 3. Different morphologies of Ti_2S nanofibers revealed by SEM: (a) quadrilateral cross-section; (b) triangular cross-section; (c) hexagonal cross-section; (d) a single fiber ending with a particle, a characteristic of VLS growth.

TEM, SEM, EDX and HRTEM. A typical TEM image of the synthesized product is shown in Figure 2. Most of the fibers are straight and smooth, while others have a wavy appearance. Further SEM analysis in Figure 3 (a–d) shows that the fibers exhibit polygonal, rather than circular, cross-sections. Different kinds of

---

(12) Lee, Y. H.; Kim, S. G.; Tomanek. *Phys. Rev. Lett.* **1997**, *78*, 2393. Journet, C.; Maser, W. K.; Bernier, A.; Loiseau, A.; Lamy, M.; Chapelle, Lamy de la.; Lefrant, S.; Deniard, P.; Lee, R.; Fisher, J. E. *Nature* **1997**, *388*, 756.

(13) Meng, G. W.; Zhang, L. D.; Qin, Y.; Phillipp, F.; Qiao, S. R.; Guo, H. M.; Zhang, S. Y. *Chin. Phys. Lett.* **1998**, *15* (9), 689.

(14) Joint Committee on Powder Diffraction Standards (JCPDS); 11–664.

cross-sections of the fibers are revealed, such as quadrilateral (a), triangular (b), and hexagonal cross-sections (c). Because the nanofibers are randomly displayed on the supported Cu microgrids, the nanofibers with cross-sections may have a different thickness along the electron beam direction, resulting in the different image contrast of the fibers in Figure 2. In addition, Figure 3d shows a fiber ending with a particle, a typical characteristic of the VLS mechanism. Further analysis by an EDX spectrometer mounted on an SEM shows that the fibers with polygonal cross-sections are Ti_2S crystals. The terminal particle mainly consists of Ni, with small amount of Ti, S, and C elements. It should be noted that the size of the fiber is about two times larger than that of real fibers due to the presputtered conducting Pt metal.

The detailed structure and composition of the individual nanostructures have been further investigated using HRTEM, SAED, and EDX. Figure 4a shows a representative image of Ti_2S fibers. The SAED pattern (inset) was recorded perpendicular to the axis of this fiber. The corresponding lattice fringes [Figure 4b] show the (002) plane perpendicular to the fiber axis with an interplanar spacing of 5.577 Å, confirming the ⟨001⟩ growth direction of the fiber. Figure 4c shows another fiber with a larger diameter (about 50 nm); the SAED pattern (inset in Figure 4c) was recorded perpendicular to the axis of this fiber, which is also parallel to the ⟨001⟩ zone axis of the hexagonal Ti_2S crystal. The (100) direction of the SAED pattern is parallel to the long axis of this fiber and thus shows that the fiber grows along the ⟨001⟩ direction, which was further confirmed by the HRTEM image in Figure 4d. After systematic examination of many fibers, we conclude that the Ti_2S fibers have a common growth axis of [001]. EDX (attached to the HRTEM) measurements made on the representative fiber revealed that only Ti, S, and Cu atoms were detected. The atom ratio of Ti/S calculated from the qualitative analysis data is about 2.07:1, which is close to that of a bulk Ti_2S phase within experiment error. The Cu atoms were generated from the Cu grid.

Growth Procedure and Mechanism. Although the Ti_2S nanofibers were clearly confirmed from the above analysis, the growth procedure of the Ti_2S nanofibers in our experiment is complicated. First, the highly dispersed $NiSO_4$ nanoparticles in the pores of activated carbon start to decompose at ca. 840 °C, the following reactions (2−4) may take place easily at a higher temperature in the reduced H_2 atmosphere.

$$NiSO_4(s) \rightarrow NiO(s) + SO_3(g) \quad (1)$$

$$NiO(s) + H_2(g) \rightarrow Ni(s) + H_2O(g) \quad (2)$$

$$SO_3(g) + 4H_2(g) \rightarrow H_2S,\ S(g) + 3H_2O(g) \quad (3)$$

$$TiCl_4(g) + (2-x/2)H_2(g) \rightarrow TiCl_x(g) + HCl_{4-x}(g) \quad (4)$$

Thus, the gaseous species of H_2S (or S vapor) and $TiCl_x$ formed with high vapor pressure. In addition, the reaction 2 generated large quantities of small Ni nanoparticles or nanoclusters. The highly active Ni catalysts provide energetically favorable sites for the deposition of Ti and S atoms from the vapor phase reactant H_2S, S, and $TiCl_x$. Furthermore, a small amount of C atoms

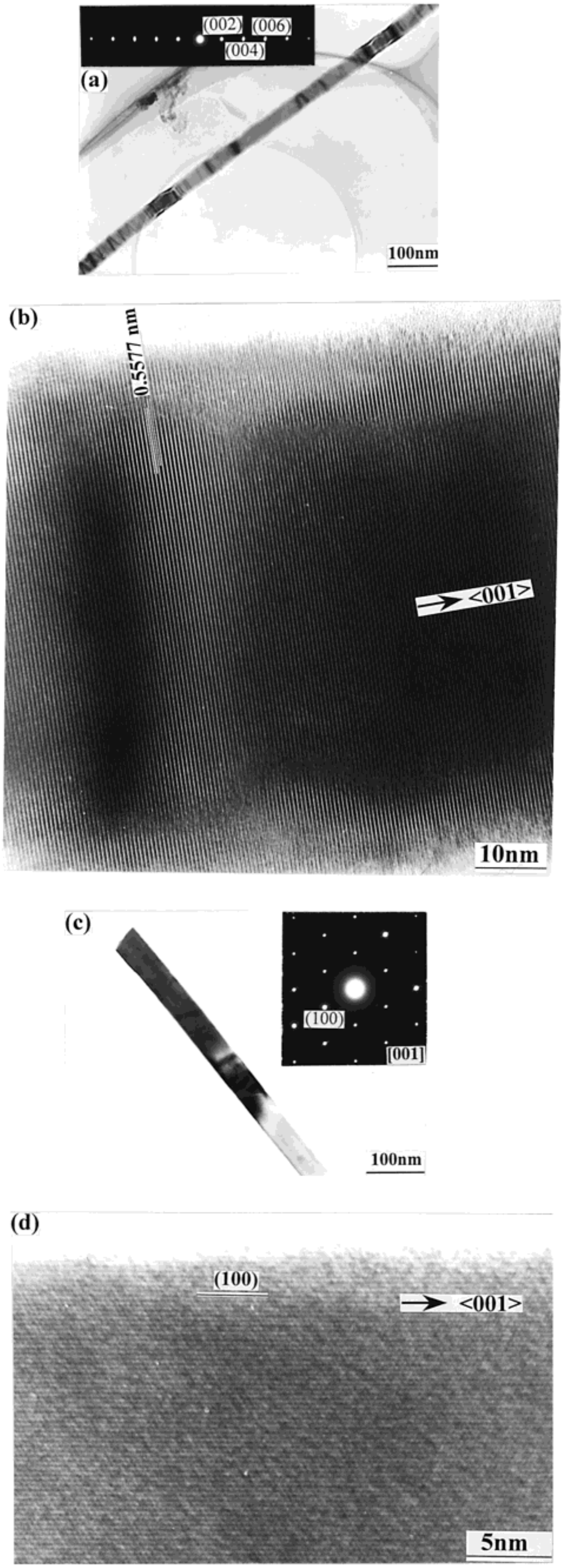

Figure 4. TEM micrographs, SAED patterns (taken perpendicular to the axis of the corresponding fiber), and the corresponding HRTEM images of Ti_2S nanofibers: (a) a ca. 30 nm diameter fiber, the inset is the SAED pattern; (b) the corresponding HRTEM image of the fiber in (a); (c) a single fiber ca. 50 nm in diameter, SAED pattern of [001] (inset); (d) a two-dimensional lattice image of the fiber in (c).

can also dissolve into the Ni catalyst by solid-state diffusion from the activated carbon cellular, though, which is rather stable at high temperature. Therefore, ultrafine Ni−Ti−S−C liquid alloys would be formed. The Ni catalyst in this liquid alloy plays a key role in the formation of Ti_2S nanofiber via the VLS mechanism. We assume that with the dissolution of Ti and S in the liquid alloy proceeding, the liquid alloy will become supersaturated preferentially with Ti and S atoms. The Ti_2S phase will be formed through reaction 5 in the form of nanofibers. At the same time, the liquid droplet is pushed upward by the proceeding fiber. The pushed liquid droplet may consist of mainly Ni, with a small amount of Ti, S, and C atoms.

$$\mathrm{Ni{-}S{-}Ti{-}C(l)} \rightarrow \mathrm{Ti_2S(s)} + \mathrm{Ni} \\ \text{(small amount of Ti, S, and C atoms)(l)} \quad (5)$$

In addition, it should be pointed out that the growth of TiC whiskers would be suppressed in our case. On one hand, it is very difficult for the liquid droplet to become supersaturated with C atoms. The reason is that only a small amount of C atoms is dissolved in Ni−S−Ti alloy, and the diffusing rate from the solid activated carbon is much smaller compared with the Ti and S atoms from vapor phases. On the other hand, the temperature is not high enough for the growth of TiC whiskers. The TiC whiskers generally form at 1300∼1450 °C and the lower deposition temperature for the formation of TiC whiskers is ca. 1125 °C by the VLS mechanism.[15] The equilibrium eutectic point of the Ni−Ti−C alloy is much higher than the temperature used in our experiment. When these are taken all together, the main feature of our synthesis route is that nanosized Ni particles are initially formed, and gas reactants of H_2S, S, and $TiCl_x$ are generated almost simultaneously, which facilitates the nucleation and the rapid growth of Ti_2S nanofibers via VLS mechanism. Further studies are required to understand the growth of Ti_2S nanofibers in detail.

Conclusions

We present a new method for the synthesis of Ti_2S nanofibers. A VLS growth mechanism is proposed for the formation of Ti_2S nanofibers at elevated temperature in a reduced H_2 atmosphere, using $TiCl_4$ and $NiSO_4$ as the starting materials. The Ni catalyst provides an energetically favored site for the absorption of gaseous species of H_2S, S, and $TiCl_x$, and then a Ti_2S nanofiber precipitates in a preferable [001] axis. Similar methods may be effective in the synthesis of other transition-metal sulfide 1D nanostructures.

Acknowledgment. The authors thank Professor L. Chen, Structure Research Laboratory, University of Science and Technology of China, Hefei, for careful investigation with XRD and Professor Y. Q. Mao, Institute of Geology and Paleontology, Chinese Academy of Sciences, Nanjing, for use of the SEM facility. This work was supported by Natural Science Foundation of China (Grant No. 19974055) and the Key Project of National Fundamental Research in Nanostructured Materials.

CM001421I

---

(15) Wokulski, Z. *J. Cryst. Growth* **1987**, *82*, 427; Kato, A.; Tamari, N. *J. Cryst. Growth* **1980**, *49*, 199; Yuan, Y.; Pan, J. *J. Mater. Sci.* **1998**, *33*, 5773.